Available online at www.sciencedirect.com
ScienceDirect
European Journal of Pharmaceutics and Biopharmaceutics 68 (2008) 760–770
European Journal of Pharmaceutics and Biopharmaceutics
www.elsevier.com/locate/ejpb

Research paper

Process design applied to optimise a directly compressible powder produced via a continuous manufacturing process

Y. Gonnissen [a], S.I.V. Gonçalves [a], B.G. De Geest [b], J.P. Remon [a], C. Vervaet [a,*]

[a] *Laboratory of Pharmaceutical Technology, Ghent University, Ghent, Belgium*
[b] *Laboratory of General Biochemistry and Physical Pharmacy, Ghent University, Ghent, Belgium*

Received 23 July 2007; accepted in revised form 14 September 2007
Available online 25 September 2007

Abstract

Manufacturing of 'ready-to-compress' powder mixtures for direct compression was performed by spray drying, without granulation, milling and/or blending steps in between spray drying and compaction. Powder mixtures containing acetaminophen, mannitol, erythritol, maltodextrin, crospovidone, colloidal silicon dioxide and polyoxyethylene 20 sorbitan monooleate were prepared via co-spray drying. A feed suspension having a solid content of 27.2% w/w was selected for further process optimisation because of its high process yield, excellent flowability and short tablet disintegration time. Experimental design was applied to evaluate processibility, physico-chemical properties and compactability of the spray dried powder mixtures. Significant and adequate regression models were developed for powder flowability, median particle size, bulk density, residual moisture content and process yield. An increasing inlet and outlet drying air temperature improved process yield. However, a higher inlet drying air temperature had a negative influence on density and moisture content, while the latter decreased at higher outlet drying air temperatures. Median particle size increased with a higher inlet temperature, while the outlet temperature had the opposite affect. Numerical optimisation determined the optimal spray drying process (inlet temperature: 221 °C, outlet temperature: 81 °C and atomisation pressure: 6 bar) in order to produce 'ready-to-compress' powder mixtures.

Keywords: Co-spray drying; Process design; Continuous processing; Acetaminophen; Carbohydrates; Compression

1. Introduction

Unlike the chemical, food, automotive and electronics industry where continuous processing has been employed for many years, conventional pharmaceutical manufacturing is generally performed using batch processing with laboratory testing conducted on collected samples to evaluate quality. The pharmaceutical industry has historically gained high profit margins and over the years limited efforts have been taken to implement time- and cost-reducing strategies and to change the manufacturing concept from batch-wise to continuous processing [1]. A change towards innovative continuous processing in the pharmaceutical industry could create regulatory uncertainty about the approval of the product. Continuous manufacturing was only able to satisfy the high quality requirements within the pharmaceutical and healthcare industry by innovative real time quality assurance using in- and on-line measurement of critical process parameters and physico-chemical properties of the manufactured goods.

Continuous processing has been preferred over batch-wise processing because of divers reasons. It reduces the time-to-market because of scale-up benefits and better quality (no batch-to-batch variations, clinical trial batches and production batches are produced on the same equipment) [1–3]. During transfer towards commercial production no bioequivalence study is demanded. Material handling is simplified since less time is required for filling, emptying and cleaning machines and a continuous process benefits from a reduced capital investment and reductions in labour costs, floor space and minimal wastage [4].

* Corresponding author. Laboratory of Pharmaceutical Technology, Ghent University, Harelbekestraat 72, 9000 Ghent, Belgium. Tel.: +32 9 2648054; fax: +32 9 2228236.
E-mail address: Chris.Vervaet@UGent.be (C. Vervaet).

0939-6411/$ - see front matter © 2007 Elsevier B.V. All rights reserved.
doi:10.1016/j.ejpb.2007.09.007

Since the traditional concept of tablet manufacturing consists of several batch-wise steps (granulation, blending, tabletting), Gonnissen et al. [5–7] developed a coprocessing technique via spray drying to be able to continuously manufacture 'ready-to-compress' mixtures, without intermediate granulation, milling or blending. Using acetaminophen as a poorly compressible drug a mixture of carbohydrates (mannitol, erythritol, maltodextrin), disintegrant (crospovidone), glidant (colloidal silicon dioxide) and surfactant (polyoxyethylene 20 sorbitan monooleate) was selected for process optimisation of 'ready-to-compress' co-spray dried powders intended for direct compression [5–7].

The purpose of this study is to optimise the solid content of the feed used for co-spray drying since this increases process capacity, while minimising energy requirements, thus improving the economical profitability. Experimental design is applied to optimise the spray drying process regarding processibility, physico-chemical properties of the spray dried powder mixtures and tablet properties in order to achieve a continuous production process for solid dosage forms containing a poorly compressible drug substance. In addition, improving the manufacturing process (solid content of the feed, spray drying parameters) could improve flow properties (flowability index, density, particle size distribution, particle shape, residual moisture content).

2. Materials and methods

2.1. Materials

Acetaminophen (D_{50}: 15 μm) was purchased from Atabay (Istanbul, Turkey). Erythritol (C*Eridex 16955) and mannitol (C*Mannidex 16700) were donated by Cerestar (Mechelen, Belgium). Maltodextrin (Glucidex® 9) was a gift from Roquette (Lestrem, France). Crospovidone (Kollidon® CL) was kindly donated by BASF (Ludwigshafen, Germany). Polyoxyethylene 20 sorbitan monooleate (Polysorbate 80) was purchased from Certa (Braine L'Alleud, Belgium). Colloidal silicon dioxide (Aerosil® 200) was obtained from Federa (Brussels, Belgium).

2.2. Methods

2.2.1. Preparation of the spray dried particles

Aqueous suspensions (Table 1) of acetaminophen, mannitol, erythritol, maltodextrin (Glucidex® 9), crospovidone (Kollidon® CL), colloidal silicon dioxide (Aerosil® 200) and polyoxyethylene 20 sorbitan monooleate (Polysorbate 80) (total solid content: 8.5%, 15.7%, 21.9% and 27.2% w/w) were prepared to evaluate the effect of the solid concentration of the feed. The feed suspensions were spray dried according to the process conditions shown in Table 2.

In addition, aqueous suspensions (total solid content: 27.2% w/w) were subjected to a process design. The spray drying process conditions of the process design experiments are listed in Table 3. Spray drying of these suspensions was performed in pilot plant Mobile Minor spray dryer (GEA NIRO, Copenhagen, Denmark). The dimensions of the drying chamber were 0.84 m cylindrical height with a diameter of 0.80 m and 60° conical base. In contrast with co-spray drying of aqueous solutions containing acetaminophen and carbohydrates [5–7] via pneumatic nozzle atomisation (two-fluid nozzle), the suspensions (Table 1) were fed to a rotary atomiser at the top of the spray dryer by means of a peristaltic pump, type 520U (Watson

Table 1
Composition of the feed suspension for the coprocessed formulations

	Concentration (% of solids content)
Acetaminophen	41.9
Mannitol	20.9
Erythritol	14.2
Maltodextrin	10.0
Crospovidone	12.0
Colloidal Silicon Dioxide	0.5
Polysorbate 80	0.5

The ratio between the different components is expressed as a percentage of the final tablet composition.

Table 2
Process conditions during spray drying in the Mobile Minor spray dryer (GEA NIRO)

Process parameters	Settings
Feed rate	Variable (g/min)
Inlet drying air temperature	220 °C
Outlet drying air temperature	80 °C
Drying gas rate	80 kg/h
Atomising air pressure	6 bar
Rotary atomiser speed	31,000 rpm

Table 3
Process parameters of the process design experiments

Run	Factors		
	A: X_1 Inlet temperature (°C)	B: X_2 Outlet temperature (°C)	C: X_3 Atomisation pressure (bar)
1	200	60	6
2	170	80	6
3	170	60	5
4	215	75	5
5	215	75	4
6	170	80	6
7	170	60	6
8	230	90	6
9	170	60	4
10	170	80	4
11	200	60	4
12	170	80	4
13	205	90	6
14	180	90	5
15	200	60	6
16	230	90	5
17	205	90	6
18	230	90	4

In addition to the variable parameters (inlet and outlet drying air temperature and atomisation pressure), each spray drying process used a drying gas rate of 80 kg/h.

Marlow, Cornwall, UK) and Marprene® tubing (inside diameter: 4.8 mm) (Watson Marlow, Cornwall, UK). If the feed is an abrasive slurry of suspended solids of varying size, a rotary atomiser is more suited as a low pressure device with large flow areas and easy incorporation of wear resistant parts for prolonged trouble-free operation [8]. The spray dryer operated in co-current air flow. The spray dried particles were collected in a reservoir attached to a cyclone, cooled down to room temperature and stored (room temperature, ambient relative humidity) prior to their characterisation and further use.

2.2.2. Experimental design

Preliminary experiments were carried out to establish appropriate ranges for the processing variables. The inlet and outlet drying air temperatures varied from 170 to 230 °C and from 60 to 90 °C, respectively, while the atomisation pressure varied between 4 and 6 bar. The lower limits of the atomisation pressure, inlet and outlet drying air temperature were chosen to avoid process problems (low yield, sticking on the dryer wall surfaces). In addition, the difference between inlet and outlet drying air temperature was fixed at 90–140 °C. A minimum of 90 °C was selected to obtain an acceptable process capacity taking into account the energy loss, while a maximum difference of 140 °C was set to avoid condensation in the dryer chamber. The upper limits of the inlet and outlet drying air temperature were limited to avoid a strong negative influence on powder flowability and density, while an atomisation pressure of 6 bar was the operationally maximum working condition of the rotary atomiser.

Because the experimental space is irregular, classical process designs such as the central composite or the Box–Behnken design could not be applied. Therefore, a D-optimal mixture design was selected [9,10]. Because interactions between the variables were expected, the following quadratic model was proposed Eq. (1):

$$Y = \beta_0 + \sum_{i=1}^{3} \beta_i X_i + \sum_{i=1}^{2} \sum_{j=i+1}^{3} \beta_{ij} X_i X_j + \sum_{i=1}^{3} \beta_{ii} X_i^2 \qquad (1)$$

where Y is the response, X_i, X_j are the set points of the process variables 'i' and 'j', respectively, and β_0, β_i, β_{ij} and β_{ii} are the coefficients.

The candidate points were chosen by the software (Design-Expert version 6.0.10, Stat-Ease Inc., Minneapolis, USA) and were: vertices (10), centers of the edges (15), constraint plane centroids (7), check points (10), interior points (22) and overall centroid (1). From the 65 candidate points, 10 runs were chosen to establish the model, 4 runs for measuring the lack-of-fit and 4 runs were replicated for the experimental error, generating a total of 18 runs. This enabled the evaluation of the appropriate regression model. Manual regression was performed. The highest order significant polynomial (significance threshold: 0.05) was selected, where only significant model terms were included without destroying the model hierarchy. Outlier-t limit was set at 3.5. The significant model was used for fitting the response. The lack-of-fit test and a normal probability plot of the residuals were performed in order to evaluate the model and to detect outliers. The models provide several comparative measures for model selection. R^2 statistics, which give a correlation between the experimental response and the predicted response, should be high for a particular model to be significant. Adjusted R^2, which gives a similar correlation after ignoring the insignificant model terms, should have good agreement with predicted R^2 for the model to be fit [11]. Predicted and adjusted R^2 should be within 0.20 of each other [12]. Contour plots for the response were drawn for determination of the optimal variable settings.

The different responses were powder flowability, median particle size, bulk density, residual moisture content, process yield, tablet tensile strength, disintegration time and friability.

2.2.3. Spray dried powder evaluation

The flowability (n: 3) (expressed as the flowability index ff_c in Eq. (2)) and bulk density (n: 3) of the powders were measured with a ring shear tester, Type RST-XS (Dietmar Schulze, Schüttgutmesstechnik, Wolfenbuttel, Germany). A detailed explanation of this technique can be found in Röck and Schwedes [13]. The powders were tested using three different consolidation stresses σ_1 (400, 1000, 1600 Pa) and a preshear of 2000 Pa. An ff_c-value below 1 indicates a non-flowing powder, between 1 and 2 a very cohesive powder, between 2 and 4 a cohesive powder, between 4 and 10 an easy flowing powder and above 10 a free flowing powder.

$$\mathrm{ff}_c = \sigma_1/\sigma_c \qquad (2)$$

where σ_1 is the consolidation stress and σ_c the unconfined yield strength (compressive strength) of a bulk solid.

The porosity of tablets composed of powder mixtures obtained via spray drying feed suspensions with different solid contents was defined using a helium gas pycnometer, Accupyc 1330 (Micromeritics, Norcross). The following analysis parameters were used: 10 purges, 10 runs and 19.5 psig as purge and run fill pressure. Final thickness and diameter of the tablets were measured with an electronic digital calliper (Bodson, Luik, Belgium).

The moisture content of the spray dried powders were determined via loss-on-drying using a Mettler LP16 moisture analyser, including an infrared dryer and a Mettler PM460 balance (Mettler-Toledo, Zaventem, Belgium). A sample of 5 g was dried at 105 °C during 15 min.

The median particle size (D_{50}) and span of each spray dried powder was determined using dry powder (jet pressure: 2.8 bar, feed rate: 2 g) laser diffraction (Mastersizer, Malvern, Worchestershire, UK).

SEM images were recorded with a Quanta 200 FEG (FEI, Eindhoven, The Netherlands) scanning electron microscope operated at an acceleration voltage of 5 kV. The powder was deposited onto a carbon carrier substrate.

In order to fluorescently label the amorphous phase of the spray dried particles FITC-dextran was added to the suspen-

sion at a 0.5% (w/w) concentration of the maltodextrin fraction in the suspension. The FITC-dextran was added to the solution of mannitol, erythritol, maltodextrin and polyoxyethylene 20 sorbitan monooleate and stirred until complete dissolution before the addition of acetaminophen, crospovidone and colloidal silicon dioxide. Confocal microscopy images of FITC-dextran labelled spray dried particles were recorded with a Nikon EZC1-si confocal microscope equipped with a 40× objective. Z-stacks were recorded over a total interval of 50 μm with a 1 μm step size.

The thermal behaviour of the binary spray dried mixtures was compared with their physical mixtures using differential scanning calorimetry. Modulated temperature DSC experiments (heating rate: 2 °C/min, modulation amplitude: 0.5 °C, modulation period: 60 s and temperature range: −20–200 °C) were performed using a DSC 2920 calorimeter (TA Instrument, New Castle, USA) with a DSC refrigerated cooling system (TA Instruments, New Castle, USA).

X-ray diffraction (D-500, Siemens, Germany) with CuK_{λ} radiation (0.154 nm) was performed. The angular range (2θ) varied from 10 to 60° with steps of 0.02° and the measuring time was 1s/step.

2.2.4. Tabletting process and evaluation

The powder mixtures were compacted on an excentric tablet press, Type EKO (Korsch, Berlin, Germany) equipped with 13.5 mm circular edged punches. The tablet properties were evaluated at a compression pressure of 74 MPa (evaluation of the solid content of the feed) or 111 MPa (process design).

Based on the diametral crushing strength of the tablets (500 ± 5 mg), determined using a hardness tester, Type PTB (Pharma Test, Hainburg, Germany), the tensile strength of the tablets (n: 10) was calculated according to Fell and Newton [14]. Tablets (n: 6) were tested for disintegration time using a disintegrator, Type PTZ (Pharma Test, Hainburg, Germany). The test was performed in 900 ml demineralised water (37.0 °C ± 0.5 °C). Tablet friability was tested on 10 tablet (n: 3) using a friabilator, Type PTF (Pharma Test, Hainburg, Germany).

3. Results and discussion

3.1. Increasing solid content

Coprocessing of acetaminophen/carbohydrate solutions has demonstrated the efficiency of mannitol, erythritol and maltodextrin to improve the physical properties and compactability of acetaminophen [5,6]. Glucidex® 9 was selected as maltodextrin type because it improved tablet disintegration in combination with acceptable physicochemical powder properties, tablet tensile strength and friability, while Kollidon® CL minimised tablet disintegration time [7]. Thus, a combination of acetaminophen, mannitol, erythritol, maltodextrin (Glucidex® 9), crospovidone (Kollidon® CL), colloidal silicon dioxide and polyoxyethylene 20 sorbitan monooleate was selected for process optimisation of 'ready-to-compress' co-spray dried powders intended for direct compression. Colloidal silicon dioxide was used as yield-increasing agent. This compound facilitates drying by its capacity to absorb large amounts of water into its pores, thus preventing sticking of semi-wet spray dried particles to the chamber walls [15]. Polyoxyethylene 20 sorbitan monooleate was included to improve the quality of the feed suspension used for co-spray drying in case of highly dosed poorly water soluble drug substance (preventing agglomeration of suspended particles and sticking to the container surface) and to decrease tablet disintegration time.

The flowability index (ff_c), bulk density, residual moisture content, process yield and median particle size as a function of solid content are mentioned in Table 4. Increasing the solid content of the feed had no significant influence on the flowability index, while bulk density changed significantly: at a higher solid content of the feed, a lower bulk density of the spray dried powders was obtained. Although the bulk density of spray dried powders also depends on the dimensions of the drying chamber, atomisation device, process conditions and feed composition, the lower residual moisture content and larger particle size observed for formulations processed at higher solid content contributed to the lower bulk density.

A higher solid content of the feed increased the median particle size due to the larger volume occupied by the solid fraction, resulting in more particle collisions and agglomeration. In addition, a higher solid content of the feed suspension increased the viscosity forming larger droplets. Similarly, the production of tomato powder from tomato paste showed an increased particle size at increasing solid content of the feed [16].

A higher solid content increased process yield, while residual moisture content of the spray dried powder mixtures was lowered. The atomisation of a concentrated feed suspension decreased the drying load since less water in a droplet needs to be evaporated. In addition, it is easier to achieve moisture removal from suspension-type droplets

Table 4
Influence of solid content of the feed on powder flowability, ff_c, (n: 3, mean ± st.dev.), bulk density (n: 3, mean ± st.dev.), residual moisture content, process yield and median particle size (D_{50}/ span)

Solid content (% w/w)	ff_c	Bulk density (g/ml)	Residual moisture content (% w/w)	Process yield (% w/w)	Median particle size (μm)
8.5	6.87 ± 0.15	0.352 ± 0.015	2.1	53.1	25.4
15.7	7.67 ± 0.31	0.338 ± 0.008	2.0	60.7	27.2
21.9	7.80 ± 0.61	0.315 ± 0.009	1.0	67.0	30.8
27.2	8.50 ± 0.89	0.326 ± 0.006	1.0	65.4	35.5

than solution-type droplets especially when the latter involve diffusion-limited film-forming characteristics at the surface [8]. Process yields mentioned in Table 4 are an underestimation as the duration of the spray drying experiments was limited to about 30 min. Processing a larger batch improved process yield as a large fraction of material is lost during the start-up phase before equilibrium process conditions are obtained: process yield increased from 65.4% to 84.1% when process time of a feed suspension at 27.2% solid content was extended from 31 to 84 min.

Tablet tensile strength and disintegration time decreased significantly with increasing solid content of the feed (Table 5) although at higher solid concentration (15.7–27.2% w/w) no significant difference in disintegration time was measured. The decrease in tensile strength and disintegration time was correlated with an increasing tablet porosity. Tablets with a high porosity are prone to rapid disintegration due to the fast water penetration into the porous network [17]. The tablet friability was independent of the solid content of the feed suspension.

A feed suspension having a solid content of 27.2% w/w was selected for further process optimisation because of its high process yield and short disintegration time in combination with excellent flowability properties. SEM picture (Fig. 1) of a spray dried powder produced via coprocessing of a concentrated feed suspension (solid content of the feed: 27.2% w/w) showed large irregular agglomerates. In addition, confocal microscopy images (Fig. 3) of a spray dried particle showed agglomerates composed of individual acetaminophen crystals with a size corresponding to the average particle size of the micronised acetaminophen (D_{50}: 15 μm) (Fig. 3).

In addition, we were interested to know how the amorphous maltodextrin compound, which acted as binding material in the formulation, was distributed throughout the spray dried particles. Therefore, in order to visualize the amorphous phase of the spray dried particles fluorescent FITC-dextran was added to the suspension. As FITC-dextran is an amorphous compound it will be distributed within the amorphous phase of the spay dried particles. Therefore this approach is well suited for the visualization (by fluorescence microscopy) of the distribution of maltodextrin in a spray dried particle since no other amorphous materials were detected on a DSC thermogram of a spray dried mixture (Fig. 2). Fig. 3 shows a

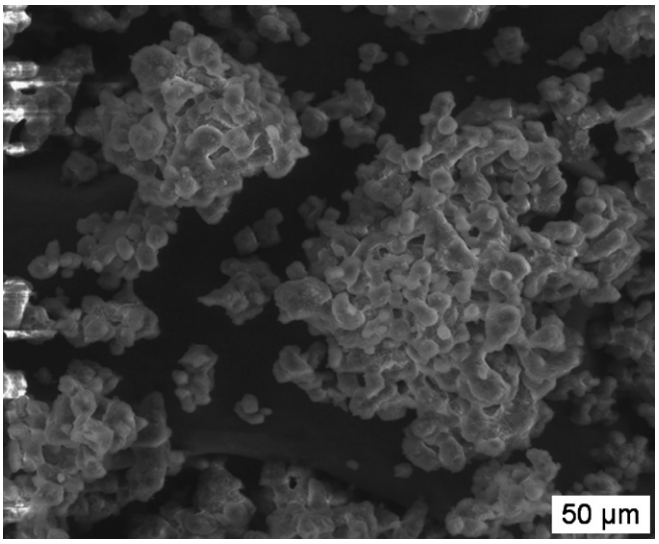

Fig. 1. SEM picture of spray dried powder (total solid content of the feed suspension: 27.2% w/w).

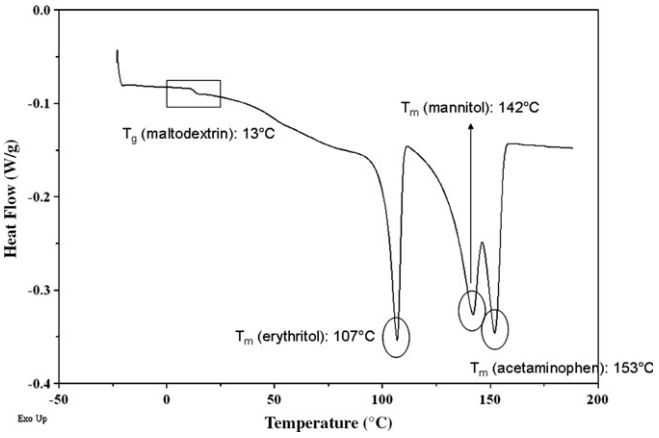

Fig. 2. Differential scanning calorimetry analysis of spray dried powder (total solid content of the feed suspension: 27.2% w/w).

Z-stack (i.e. a stack of confocal images taken at different heights through the sample) of a spray dried particle. The sequence of the images is from top (0 μm) to bottom (40 μm). As can be observed in Fig. 3 the fluorescence is distributed throughout the spray dried particle, indicating that amorphous maltodextrin is spread throughout the entire spray dried particle (taking into account the variation of fluorescence at the top and bottom because of the irregular shape of the spray dried particle).

Table 5
Influence of solid content of the feed on tablet porosity, tablet tensile strength (n: 10, mean ± st.dev.), tablet disintegration time (n: 6, mean ± st.dev.) and tablet friability (n: 3, mean ± st.dev.)

Solid content (% w/w)	Tablet porosity (%)	Tensile strength (MPa)	Friability (%)	Disintegration time (min)
8.5	18.0	1.53 ± 0.10	0.88 ± 0.08	7.0 ± 1.0
15.7	22.8	1.20 ± 0.11	1.10 ± 0.19	2.9 ± 0.1
21.9	23.4	1.05 ± 0.04	1.12 ± 0.04	2.4 ± 0.5
27.2	24.1	0.95 ± 0.06	1.19 ± 0.15	2.0 ± 0.1

Compression pressure: 74 MPa.

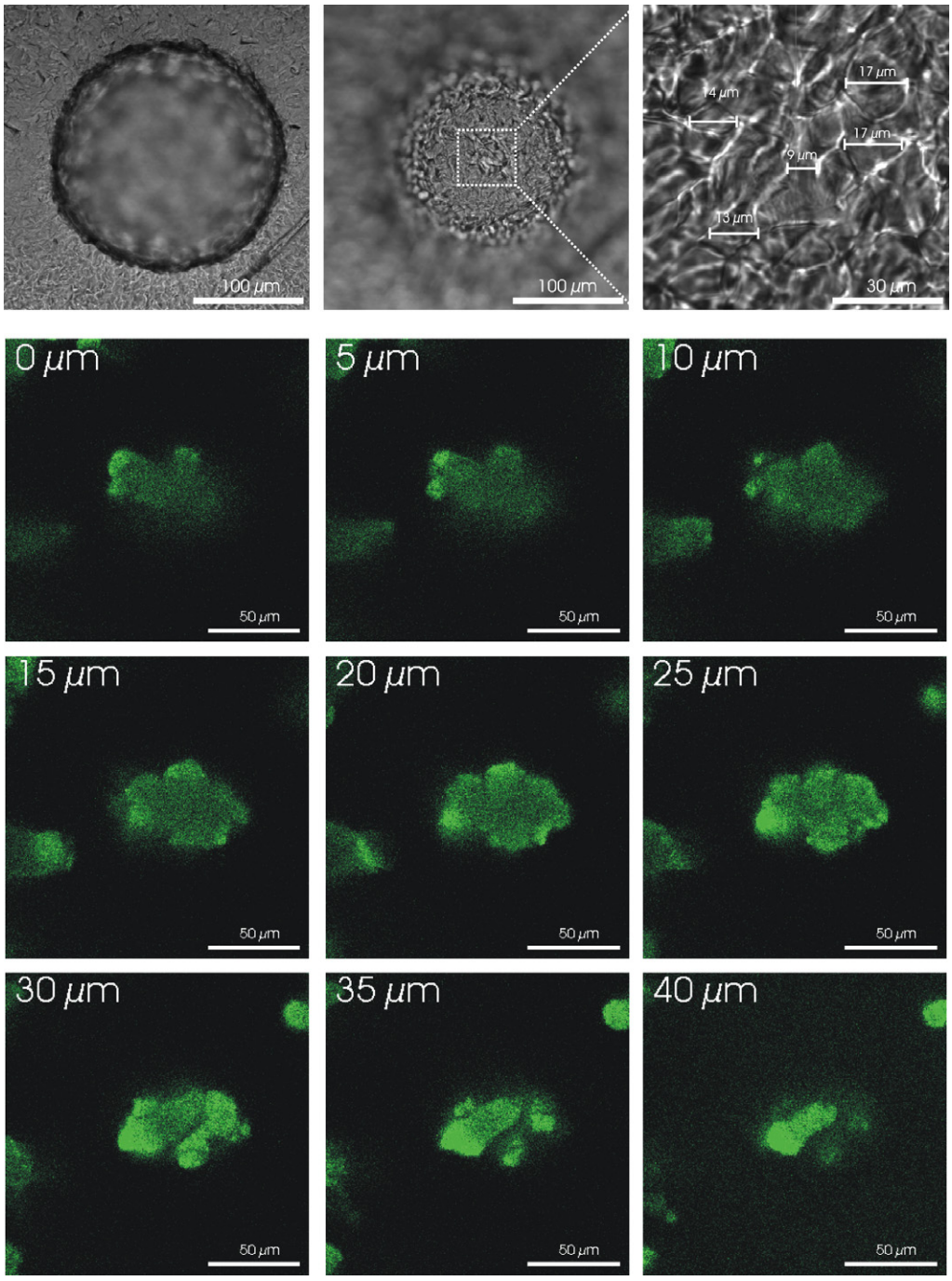

Fig. 3. Confocal microscopy images of spray dried particle (top) and fluorescently labelled spray dried particle (bottom) (total solid content of the feed suspension: 27.2% w/w).

Fig. 4 shows the X-ray diffraction spectra of pure acetaminophen, mannitol, erythritol, maltodextrin and the spray dried powder (Table 1). Pure acetaminophen and acetaminophen in the spray dried powder mixture were of crystalline nature as identical sharp peaks were observed in both the diffraction patterns (e.g. 2θ: 18.2°, 24.3°, 26.6° and 32.8°). In addition, pure erythritol and mannitol were crystalline as indicated by numerous distinct peaks. The prominent peaks from pure erythritol (2θ: 19.8° and 28.3°) and pure mannitol (2θ: 18.8°, 23.4° and 44.1°) were also present in the diffraction spectrum of the spray dried powder. Maltodextrin was found to be amorphous, as indicated by the absence of diffraction peaks.

3.2. Process optimisation design

3.2.1. Summary statistics for the model

Analysis of variance of the responses (Table 6) indicated that response surface models developed for powder flow-

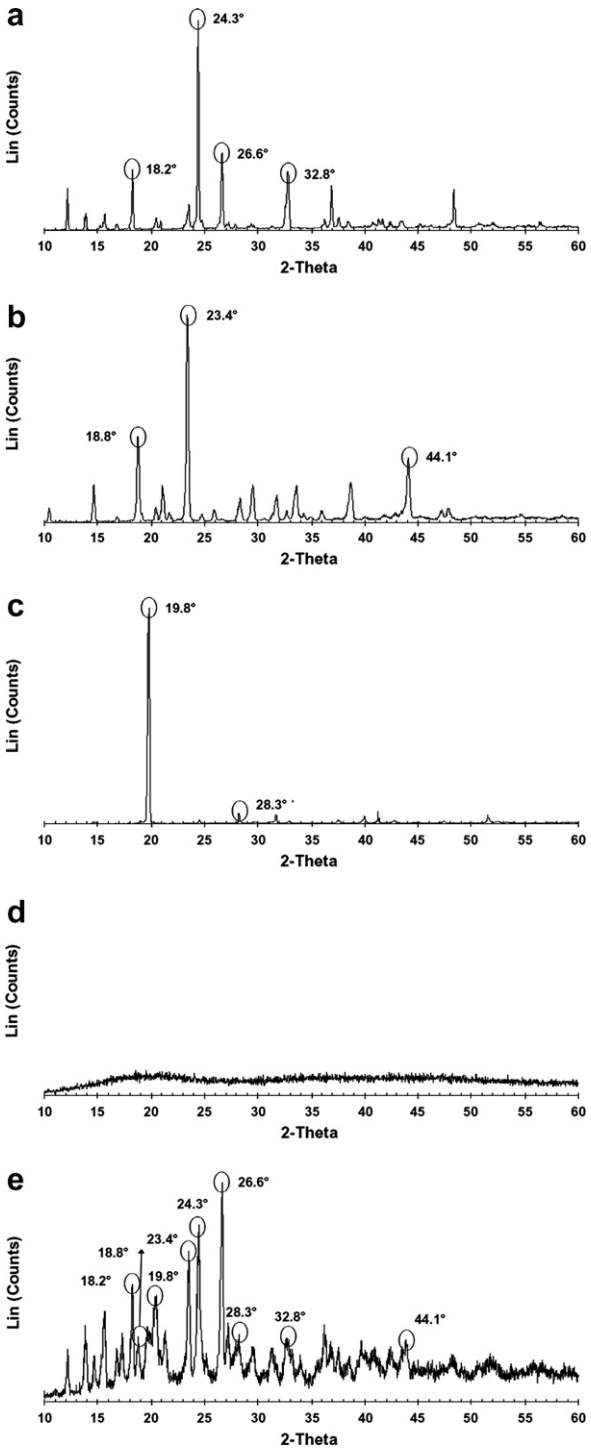

Fig. 4. X-ray diffraction patterns of acetaminophen (a) mannitol (b), erythritol (c), maltodextrin (d) and the spray dried powder mixture (total solid content of the feed suspension: 27.2% w/w) (e).

ability, median particle size, density, residual moisture content process yield, tablet tensile strength, disintegration time and friability were significant, without significant lack of fit. Transformation of median particle size (power transformation, λ: −2.54) response was needed because the residuals were a function of the magnitude of the predicted values.

Table 6
ANOVA – influence of spray drying process variables on the response factors

Response factor	Model *F*-value	Prob > *F*	Lack of Fit *F*-value	Prob > *F*
Flowability	45.92	<0.0001	0.58	0.7798
Median particle size (D_{50}) (μm)	73.54	<0.0001	0.33	0.9284
Density (g/ml)	30.27	<0.0001	1.49	0.3743
Moisture content (%)	57.99	<0.0001	0.91	0.5976
Spray drying yield (%)	45.92	<0.0001	0.58	0.7798
Tablet tensile strength (MPa)	4.21	0.0275	0.76	0.6025
Tablet disintegration time (s)	5.68	0.0113	0.72	0.6197
Tablet friability (%)	4.25	0.0185	1.77	0.3029

Table 7 details the model summary statistics for the selected significant models. It can be observed that, with exception of tablet tensile strength, disintegration and friability, R^2, predicted R^2 and adjusted R^2 are in good agreement, resulting in reliable models.

Moreover, the effect of process design variables on tablet properties is not of major importance, since tablet tensile strength, disintegration time and friability of all process design runs were within acceptable ranges (>1.10 MPa, <5 min and <0.70%, respectively) (Table 8). The developed regression models for tablet tensile strength, disintegration time and friability did not evidence acceptable statistical measures.

3.2.2. Flowability

Flowability index (ff_c) is a measure of the flow properties of spray dried powder mixtures. The powder flowability of run 9 was classified as an outlier. Powder flowability is predicted by a 2-factor interaction model. Run 3 and 7 produced at low drying air temperatures (inlet temperature: 170 °C, outlet temperature: 60 °C) had a higher flowability index in comparison with formulations co-spray dried at high drying air temperatures (inlet temperature: 230 °C, outlet temperature: 90 °C for run 8, 16 and 18) (Table 9).

Table 7
Model summary statistics – influence of spray drying process variables on the response factors

Response factor	St.dev.	R^2	Adjusted R^2	Predicted R^2
Flowability	3.36	0.9077	0.8880	0.8576
Median particle size (D_{50}) (μm)	1.039E-005	0.9403	0.9275	0.9012
Density (g/ml)	7.012E-003	0.8122	0.7854	0.7220
Moisture content (%)	0.44	0.8855	0.8702	0.8376
Spray drying yield (%)	3.36	0.9077	0.8880	0.8576
Tablet tensile strength (MPa)	0.11	0.8258	0.6298	0.1163
Tablet disintegration time (s)	22.50	0.8647	0.7124	0.2497
Tablet friability (%)	0.088	0.6988	0.5346	0.1499

Table 8
Response results (tablet tensile strength (n: 10, mean ± st.dev.), tablet disintegration time (n: 6, mean ± st.dev.) and tablet friability (n: 3, mean ± st.dev.)) for process design

Run	Responses		
	Tablet tensile strength (MPa)	Tablet disintegration time (s)	Tablet friability (%)
1	1.11 ± 0.06	134 ± 9	0.58 ± 0.18
2	1.47 ± 0.04	245 ± 63	0.57 ± 0.05
3	1.84 ± 0.06	295 ± 4	0.51 ± 0.07
4	1.37 ± 0.05	218 ± 12	0.66 ± 0.02
5	1.35 ± 0.05	215 ± 9	0.68 ± 0.04
6	1.52 ± 0.08	249 ± 16	0.54 ± 0.01
7	1.50 ± 0.03	208 ± 10	0.62 ± 0.05
8	1.35 ± 0.03	194 ± 11	0.44 ± 0.09
9	1.59 ± 0.08	267 ± 26	0.50 ± 0.03
10	1.34 ± 0.04	212 ± 21	0.23 ± 0.08
11	1.15 ± 0.06	205 ± 24	0.54 ± 0.06
12	1.57 ± 0.07	220 ± 14	0.30 ± 0.08
13	1.37 ± 0.03	225 ± 22	0.36 ± 0.05
14	1.63 ± 0.06	288 ± 17	0.45 ± 0.09
15	1.31 ± 0.11	164 ± 21	0.58 ± 0.09
16	1.44 ± 0.04	241 ± 18	0.33 ± 0.11
17	1.45 ± 0.06	292 ± 14	0.55 ± 0.15
18	1.28 ± 0.04	248 ± 20	0.65 ± 0.15

Compression pressure: 111 MPa.

The fitted response surface model in terms of coded factors for the flowability index (ff_c) was:

$$ff_c = 7.41 - 0.50 * A - 0.39 * B - 0.24 * C + 0.91 * AB + 0.31 * AC + 0.47 * BC \quad (3)$$

where A is the inlet temperature, B is the outlet temperature and C is the atomisation pressure.

The contour plot based on Eq. (3) is given in Fig. 5.

3.2.3. Median particle size

At constant inlet drying air temperature (170 °C) the median particle size was decreased by increasing outlet drying air temperature (e.g. run 3, 7 and 9 versus run 2, 6, 10 and 12) (Table 9). In addition, coprocessing via spray drying at constant outlet drying air temperature yielded powders with larger median particle size at a higher inlet drying air temperature (run 1, 11, 15 versus run 3, 7, 9 at constant outlet drying air temperature of 60 °C). This has also been observed before. Although the effect of temperature on particle size is reported to be dependent on the material being dried [18], similar observations have been made by Ståhl et al. [19] during spray drying of insulin. Broadhead et al. [20] suggested that the increase in particle size might be an effect of increased agglomeration at the higher inlet drying air temperatures due to a higher feed rate (required to obtain a constant outlet drying air temperature if the inlet drying air temperature is increased). Atomisation pressure had no significant influence on the median particle size of the spray dried powders.

The fitted response surface model in terms of coded factors for the median particle size (D_{50}) was:

$$(D_{50})^{-2.54} = 1.124\text{E}-004 - 2.750\text{E}-005 * A + 3.580\text{E}-005 * B - 3.521\text{E}-005 * B^2 \quad (4)$$

where A is the inlet temperature and B is the outlet temperature.

The contour plot based on Eq. (4) is given in Fig. 6.

3.2.4. Powder bulk density

Bulk density of run 3 was classified as an outlier. Run 2, 6, 7, 9, 10 and 12 produced at an inlet drying air temperature of 170 °C had a significantly higher bulk density in

Table 9
Response results (powder flowability: ff_c (n: 3, mean ± st.dev.), bulk density (n: 3, mean ± st.dev.), residual moisture content, process yield and median particle size (D_{50}/ span) for process design experiments

Run	Responses				
	ff_c	Bulk density (g/ml)	Residual moisture content (% w/w)	Process yield (% w/w)	Median particle size (μm)
1	7.27 ± 0.15	0.314 ± 0.002	4.10	53.5	58.0/ 3.5
2	6.50 ± 1.32	0.346 ± 0.000	1.05	60.1	31.6/ 3.5
3	9.23 ± 0.55	0.372 ± 0.004[a]	2.49	34.2	46.2/ 3.0
4	6.67 ± 2.06	0.315 ± 0.002	1.29	63.6	36.4/ 2.9
5	7.30 ± 0.26	0.316 ± 0.002	1.43	65.1	37.1/ 3.1
6	7.37 ± 0.29	0.350 ± 0.001	1.61	49.5	33.3/ 3.7
7	8.17 ± 0.31	0.345 ± 0.003	2.91	35.0	42.4/ 3.9
8	7.70 ± 0.36	0.313 ± 0.003	0.88	57.6	40.8/ 2.9
9	7.83 ± 0.31[a]	0.328 ± 0.002	3.09	35.2	42.1/ 3.9
10	7.80 ± 0.46	0.338 ± 0.001	1.21	50.0	32.8/ 3.4
11	8.60 ± 0.85	0.313 ± 0.002	4.00	49.8	55.5/ 3.7
12	7.87 ± 0.83	0.354 ± 0.001	0.91	50.0	32.6/ 4.0
13	7.77 ± 1.07	0.319 ± 0.001	0.60	61.0	38.4/ 2.7
14	6.83 ± 0.45	0.334 ± 0.001	0.00	58.4	32.4/ 3.1
15	7.13 ± 0.15	0.316 ± 0.002	2.98	53.4	48.9/ 3.2
16	7.53 ± 0.32	0.320 ± 0.003	0.96	57.0	42.1/ 2.8
17	7.43 ± 0.21	0.315 ± 0.002	0.49	65.3	34.4/ 2.8
18	6.93 ± 0.21	0.308 ± 0.002	1.04	62.4	39.8/ 3.3

[a] Identified as outlier.

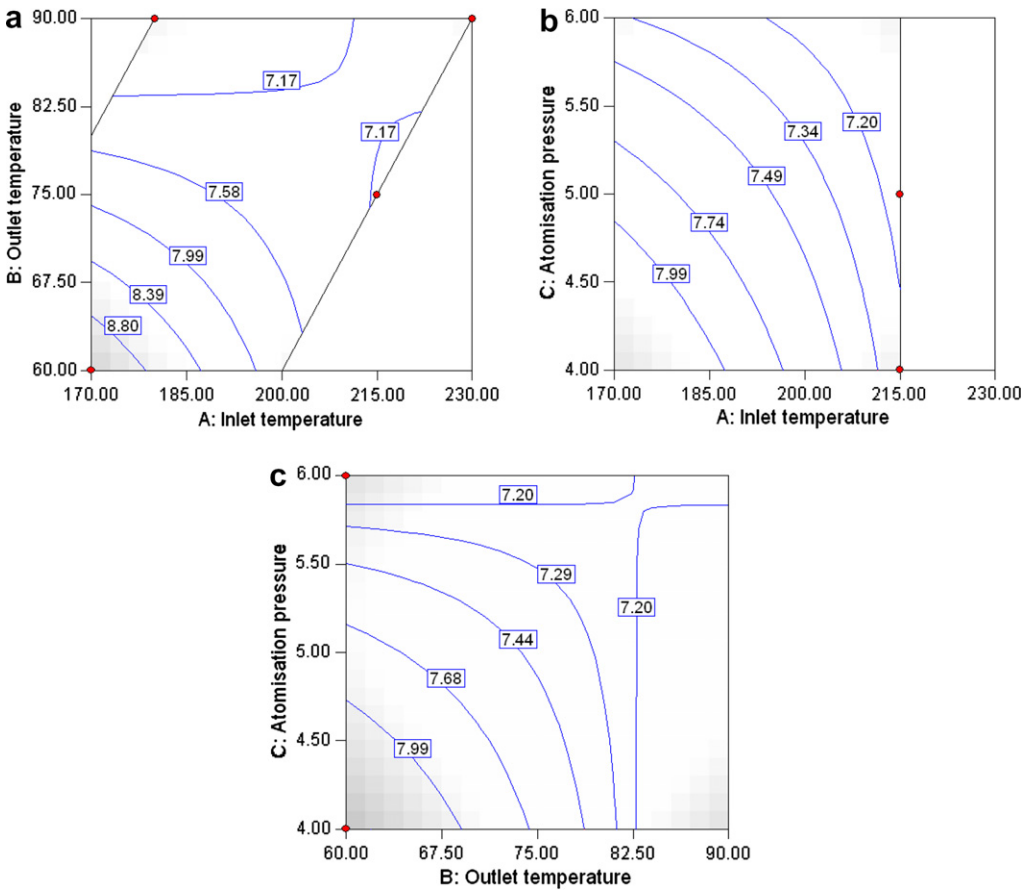

Fig. 5. Contour plots for flowability, atomisation pressure is constant at 5 bar (a), outlet temperature is constant at 75 °C (b) and inlet temperature is constant at 200 °C (c).

comparison with formulations coprocessed at medium (200 °C for run 1, 11 and 15) and high (230 °C for run 8, 16, 18) inlet drying air temperature (Table 9). Atomisation pressure had no significant influence on the bulk density of the spray dried powders. The decrease in bulk density with increasing inlet drying air temperature was due to case hardening of the droplet at higher temperatures followed by expansion of the entrapped air [21]. An increase in inlet drying air temperature decreased powder bulk density for many feed formulations but the extent was product dependent [8].

The fitted response surface model in terms of coded factors for the bulk density (BD) was:

$$BD = 0.32 - 0.019 * A + 5.677\text{E} - 003 * B \quad (5)$$

where A is the inlet temperature and B is the outlet temperature.

The contour plot based on Eq. (5) is given in Fig. 6.

3.2.5. Moisture content

Runs 1, 3, 7, 9, 11 and 15 dried at low outlet drying air temperature (60 °C) had significantly higher moisture contents compared with powders produced at medium (run 4 and 5) and high (run 8, 13, 14, 16, 17 and 18) outlet drying air temperature (Table 9). The high moisture content at low outlet drying temperature was often linked to agglomerated and sticky spray dried products. The small drying chamber of the Mobile Minor spray dryer used in this study is more prone to these problems at low drying temperatures. At constant outlet drying air temperature the moisture content was increased by the inlet drying air temperature, especially at low outlet drying air temperatures (e.g. run 7 and 9 versus run 1 and 11 at an outlet drying air temperature of 60 °C in comparison with run 13 and 17 versus run 8, 16, 18 at an outlet drying air temperature of 90 °C). In addition, Ersus and Yurdagel [22] stated that increased drying air temperatures reduced the residual moisture content, when the difference between inlet and outlet drying air temperature was constant. Atomisation pressure had no significant influence on the moisture content of the spray dried powders.

The fitted response surface model in terms of coded factors for the residual moisture content during spray drying (RMC) was:

$$\text{RMC} = 1.89 + 0.34 * A - 1.45 * B \quad (6)$$

where A is the inlet temperature and B is the outlet temperature.

The contour plot based on Eq. (6) is given in Fig. 6.

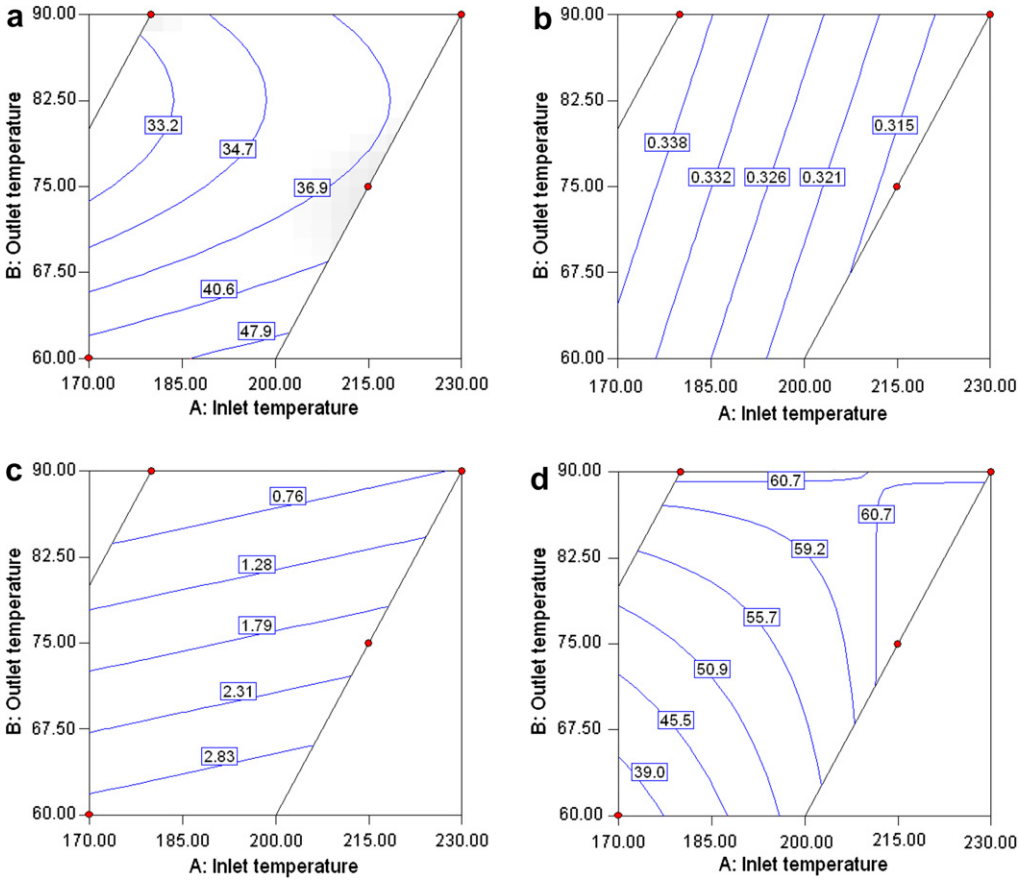

Fig. 6. Contour plots for median particle size (a), density (b), residual moisture content (c) and process yield (d) (Atomisation pressure: 5 bar).

3.2.6. Spray drying yield

Formulations prepared at low outlet drying air temperature (60 °C) had significantly lower process yields compared to compositions dried at higher outlet drying temperatures (80 °C) using similar inlet drying air temperatures (e.g. run 3, 7 and 9 versus run 2, 6, 10 and 12 at an inlet drying air temperature of 170 °C) (Table 9). At constant outlet drying air temperature (60 °C) the spray drying yield increased with increasing inlet drying air temperature as more thermal energy was provided for the immediate evaporation of the solvent. Broadhead et al. [20] showed that during spray drying of β-galactosidase the process yield was increased by increasing inlet drying air temperature. Similarly, spray drying of insulin for inhalation resulted in higher process yields at increasing inlet drying air temperature [19]. At high outlet drying air temperature (90 °C) the yield was not significantly affected by inlet drying air temperature (e.g. run 8, 13, 14, 16, 17, 18). Atomisation pressure had no significant influence on the process yield.

The fitted response surface model in terms of coded factors for the process yield (PY) was:

$$PY = 57.20 + 9.28 * A + 3.72 * B - 9.84 * AB \quad (7)$$

where A is the inlet temperature and B is the outlet temperature.

The contour plot based on Eq. (7) is given in Fig. 6.

3.2.7. Process optimisation and validation

Numerical optimisation was performed using statistical models to find the optimal spray drying process. For optimisation of the process the following targets were set: the residual moisture content must be minimised while process yield must be maximised.

According to the statistical prediction the optimal formulation process parameters were:

Inlet temperature: 221 °C

Outlet temperature: 81 °C

Atomisation pressure: 6 bar

An experiment was performed for the selected process. In addition, point predictions were constructed by entering optimal process parameters into the current model. Design-Expert software package (version 6.0.10, Stat-Ease, Minneapolis, USA) then calculated the expected responses and associated confidence and prediction intervals (Table 10) based on the prediction equations (Eqs. (3)–(7)). The prediction interval has a wider spread than the confidence interval since more scatter can be expected in individual values than in averages. All the observed results (Table

Table 10
Observed responses and point prediction of the optimal spray drying process (Inlet temperature, 221 °C; outlet temperature, 81 °C; atomisation pressure, 6 bar)

Response factor	Observed	Predicted	95% Confidence interval		95% Prediction interval	
			Low	High	Low	High
Flowability	8.77	7.32	6.93	7.71	6.52	8.11
Median particle size (D_{50}) (μm)	35.44	37.30	35.73	39.16	34.19	41.73
Density (g/ml)	0.330	0.312	0.310	0.320	0.300	0.330
Moisture content (%)	1.02	1.55	1.21	1.89	0.55	2.55
Spray drying yield (%)	63.09	62.4	59.74	65.12	54.74	70.11

10) of the measured responses were within the prediction intervals (with exception of powder flowability).

4. Conclusions

Economical profitability was improved by increasing the solid content of the feed suspension (27.2% w/w) resulting in a high process yield, excellent flowability and short tablet disintegration time. Regression models were developed for powder bulk density, moisture content and spray drying process yield. However, the atomisation pressure had no significant influence on the process yield, moisture content and density. In addition, modelling of tablet hardness, friability and disintegration time was unreliable. The optimised spray drying process had an atomisation pressure of 6 bar and an inlet and outlet drying air temperature of 221 and 81 °C, respectively. These process settings were selected for process scale-up in order to manufacture 'ready-to-compress' powder mixtures via continuous spray drying.

References

[1] C. Vervaet, J.P. Remon, Continuous granulation in the pharmaceutical industry, Chem. Eng. Sci. 60 (2005) 3949–3957.
[2] M. Leuenberger, New trends in the production of pharmaceutical granules: batch versus continuous processing, Eur. J. Pharm. Biopharm. 52 (2001) 289–296.
[3] M. Leuenberger, New trends in the production of pharmaceutical granules: the classical batch concept and the problem of scale-up, Eur. J. Pharm. Biopharm. 52 (2001) 279–288.
[4] N.O. Lindberg, Some experience of continuous granulation, Acta Pharm. Suec. 25 (1988) 289–296.
[5] Y. Gonnissen, J.P. Remon, C. Vervaet, Development of directly compressible powders via co-spray drying, Eur. J. Pharm. Biopharm. 67 (2007) 220–226.
[6] Y. Gonnissen, J.P. Remon, C. Vervaet, Mixture design applied to optimise a directly compressible powder produced via co-spray drying, Drug Dev. Ind. Pharm. Accepted 12 Jun 2007.
[7] Y.Gonnissen, J.P. Remon, C. Vervaet, Effect of maltodextrin and superdisintegrant in directly compressible powder mixtures prepared via co-spray drying, Eur. J. Pharm. Biopharm., in press, doi:10.1016/j.ejpb.2007.09.004.
[8] K. Masters, Spray Drying in Practice, SprayDryConsult Intl ApS, Denmark, 2002.
[9] G.A. Lewis, M. Chariot, Non classical experimental designs in pharmaceutical formulation, Drug Dev. Ind. Pharm. 17 (1991) 1551–1570.
[10] A. Bodea, S.E. Leucata, Optimization of hydrophilic matrix tablets using a D-optimal design, Int. J. Pharm. 153 (1997) 247–255.
[11] C.R. Hicks, K.V. Turner, Fundamental Concepts in the Design of Experiments, Oxford University Press, England, 1999.
[12] Manual Design-Expert version 6.0.10, Stat-Ease Inc., Minneapolis, USA.
[13] M. Röck, J. Schwedes, Investigations on the caking behaviour of bulk solids-macroscale experiments, Powder Technol. 157 (2005) 121–127.
[14] J.T. Fell, J.M. Newton, The tensile strength of lactose tablets, J. Pharm. Pharmacol. 20 (1968) 657–658.
[15] A. Billon, B. Bataille, G. Cassanas, M. Jacob, Development of spray-dried acetaminophen microparticles using experimental designs, Int. J. Pharm. 203 (2000) 159–168.
[16] S. Al-Asheh, R. Jumah, F. Banat, S. Hammad, The use of experimental factorial design for analysing the effect of spray dryer operating variables on the production of tomato powder, Food Bioprod. Process. 81 (C2) (2003) 81–88.
[17] M. Sugimoto, S. Narisawa, K. Matsubara, H. Yoshino, M. Nakano, T. Handa, Effect of formulated ingredients on rapidly disintegrating oral tablets prepared by the crystalline transition method, Chem. Pharm. Bull. 54 (2) (2006) 175–180.
[18] E.J. Crosby, W.R. Marshall, Effects of drying conditions on the properties of spray dried particles, Chem. Eng. Prog. 54 (1958) 56–63.
[19] K. Ståhl, M. Claeson, P. Lilliehorn, H. Lindén, K. Bäckström, The effect of process variables on the degradation and physical properties of spray dried insulin intended for inhalation, Int. J. Pharm. 233 (2002) 227–237.
[20] J. Broadhead, S.K.E. Rouan, I. Hau, C.T. Rhodes, The effect of process and formulation variables on the properties of spray dried β-galactosidase, J. Pharm. Pharmacol. 46 (1994) 458–467.
[21] H. Wallman, H.A. Blyth, Product control in Bowen-type spray dryer, Ind. Eng. Chem. 43 (6) (1951) 1480–1486.
[22] S. Ersus, U. Yurdagel, Microencapsulation of anthocyanin pigments of black carrot by spray drier, J. Food Eng. 80 (2007) 805–812.